Available online at www.sciencedirect.com
ScienceDirect
Polymer 48 (2007) 2520–2525
polymer
www.elsevier.com/locate/polymer

Polymer Communication

# Preparation and mechanical characterization of artificial hollow tubes

R. Mueller [a], L. Daehne [b], A. Fery [a,*]

[a] Max Planck Institute of Colloids and Interfaces, Wissenschaftspark Golm, 14424 Potsdam, Germany
[b] Capsulution Nanoscience AG, Volmer Str. 7b, 12489 Berlin, Germany

Received 24 November 2006; received in revised form 1 March 2007; accepted 8 March 2007
Available online 13 March 2007

**Abstract**

In this paper, we present a novel route to prepare hollow tubes using the template assisted Layer-by-Layer technique. A readily available glass fibre template was coated with polyelectrolyte multilayers, followed by subsequent fibre dissolution. After the fibre dissolution we discovered stable hollow tubes or observed a pearling instability depending on the composition of the multilayer. Here we focus on hollow tubes: we precisely characterized the tubes with Fluorescence Microscopy, Confocal Laser Scanning Microscopy and AFM Topography Imaging. The tubes have an aspect ratio of around 10, with diameters from 5 μm up to 17 μm. The Layer-by-Layer technique allows us to control the tubes' wall thickness within a few nanometers; here the total wall thickness was 60 nm. Because the tubes can find a possible application in drug delivery, we tested the permeability of the multilayer membrane. The mechanical properties of the wall were investigated with AFM Force Spectroscopy and because continuum mechanical models apply to this system we derived a Young's modulus of the wall material.


*Keywords:* Tube; Polyelectrolyte multilayer; Mechanical properties

## 1. Introduction

There are various ways to produce tube-like structures. Previously, tubes have been formed by pure self assembly. A few most prominent examples of materials used include carbon [1,2], boronitrate [3], lipid surfactants [4], or polypeptides [5]. More recently, methods for tube preparation based on template assisted self assembly have caught increasing attention due to the potential for tailoring the tubes' shape and wall thickness. Both mesoporous materials and fibres, which are dissolved after the formation of tubular coatings, can serve as templates. In the first case, coatings are formed by wetting: if interfacial interactions are suitable, then pore walls are covered by a thin wetting film, which turns into a glassy polymer film upon solvent evaporation [6].

In the second case, fibres are coated using chemical vapour deposition [7,8], or recently by Layer-by-Layer self assembly [9]. The Layer-by-Layer method was first introduced by Decher and coworkers [10] and uses the alternating adsorption of charged polymers onto an oppositely charged template surface to form a polymeric multilayer. Each adsorption step leads to a charge inversion and thus the next layer of charged polymer can be assembled onto the coated template. As detailed in several recent reviews [11–13] on this subject, the total layer thickness can be controlled with nanometer precision and various substances can be incorporated into the layers such that the multilayers can, for example, be optically functional [14] or biocompatible [15,16,11]. The solid wire or hollow tubes have diameters in the micrometer and sub-micrometer range, and their length can be up to several centimeters (electrospun fibres). Because they offer a large surface area combined with low weight and are relatively easily assembled to meshes or fleeces [17–19], these tubes have potential applications in catalysis [18], filtration [17], sensing [20], and tissue engineering [15,21]. A recent review on the various applications of freestanding nanostructures made by multilayer assembly can be found in Ref. [22]. Micromanipulation or switchable optical properties of tubes are possible

* Corresponding author. Tel.: +49 331 567 9204; fax: +49 331 567 9102.
*E-mail address:* andreas.fery@mpikg-golm.mpg.de (A. Fery).

0032-3861/$ - see front matter © 2007 Elsevier Ltd. All rights reserved.
doi:10.1016/j.polymer.2007.03.022

because due to their anisotropic shape, they can be oriented by external fields [23,24]. Finally, tubes can mechanically reinforce microstructures, as seen by one function of tube-like fibres in biological systems (protein nanotubes, microtubule) [25]. Therefore, there is a large interest towards producing tubes with micron scale lateral dimensions and submicron wall thickness.

Here we both present a simple, but novel strategy for micro-tube preparation that is based on template assisted Layer-by-Layer assembly on readily available glass fibres and show that we can produce micro-tubes with controlled geometry (diameter, length, wall thickness and aspect ratio). For the first time the permeability of these tubes and their mechanical properties are investigated with methods that allow probing these properties on a single tube basis. Substances can be encapsulated in (closed) tubes for drug delivery similar to applications shown for polyelectrolyte capsules [16]. Open tubes could be used for transport purposes or as channels in micro-fluidics.

## 2. Experimental section

### 2.1. Materials

All chemicals were purchased from Sigma–Aldrich. The polyelectrolytes used were: poly(ethylene imine) (PEI, $M_w = 25\,000$), poly(allylamine hydrochloride) (PAH, $M_w = 15\,000$), poly(styrenesulfonate) (PSS, $M_w = 70\,000$), poly(diallyldimethylammonium chloride) (PDADMAC, $M_w = 200\,000$–$350\,000$). The concentration of polyelectrolytes in the 0.2 M NaCl solution was 1 g/L and the pH was adjusted to 5.6 using a 0.02 M acetate buffer. The 0.02 M acetate buffer was prepared from acetic acid. In order to monitor the multilayer build up, PAH and PSS were labelled with Rhodamine B. Furthermore the dyes Rhodamine B ($M_w = 479.01$) and FITC labelled dextran ($M_w = 500\,000$, concentration: 3.25 mg/mL) were used.

As templates for the Layer-by-Layer process, glass fibres (diameter 5–10 μm, Uralita, Spain) were used. Prior to coating, the templates were cut with a homogeniser (Ultra Turrax/Diax 900, Buddeberg, Germany) and activated by means of a basic RCA treatment (caution: highly corrosive!): the tubes are immersed into a solution containing 5 parts $H_2O$, 1 part $NH_3$ and 1 part $H_2O_2$ at 70 °C for 10 min and thoroughly rinsed with pure Milli-Q water afterwards. After coating the templates, they were dissolved in 1 M hydrofluoric acid, HF (caution: toxic and extremely harmful!).

### 2.2. Experimental methods

#### 2.2.1. Fluorescence Microscopy

Optical images of the tubes were obtained with a Fluorescence Microscope Axiovert 200 (Zeiss, Germany) using a 63×/1.4 oil immersion objective. A drop of the sample solution was put on clean glass slide that was previously coated with a layer of PEI. The radii of at least 35 tubes were analyzed.

#### 2.2.2. Confocal Laser Scanning Microscopy

To visualize the tubes in water a Confocal Laser Scanning Microscope (Leica TCS SP and Leica CLSM SP1, Germany) was used with a 40×, 63× and 100×/1.4 oil immersion objective. The tubes can be easily detected due to the Rhodamine labelled PAH or PSS layers in the wall.

#### 2.2.3. Scanning Force Microscopy (SFM)

The topographic measurements were performed in air and at room temperature with a Nanoscope III Multimode SFM (Digital Instruments Inc.). The sample was prepared by placing a drop of the sample solution onto a silicon wafer. The silicon was cleaned with RCA previously. After the evaporation of the water in the sample solution, the tubes collapse on the silicon and the thickness of the wall was measured at the step *collapsed tube – silicon*. At least 20 profiles were analyzed.

#### 2.2.4. AFM Force Spectroscopy

Force Spectroscopic measurements were carried out under water using a commercial AFM setup NanoWizard (JPK Instruments, Germany). In this setup an AFM head is placed on an optical microscope Axiovert 200 (Zeiss, Germany) such that Fluorescence Microscopy can be used to locate and monitor the Rhodamine labelled tubes in the experiment. For the measurement a conventional pyramidal tip (CSC12/AIBS/50, MicroMash, Estonia) and the colloidal probe technique were used [26,27]: a glass bead (diameter 30–50 μm, Polyscience Inc.) is attached to a tipless cantilever (MicroMash, Estonia) with a two component epoxy clue (UHU Plus endfest 300, UHU GmbH & Co. KG, Germany) by using a micromanipulator (Suttner Instruments Co.). According to previous work [28], both tips produce the same force–deformation characteristics as long as the deformations of the shell are in the order of its wall thickness. The spring constant of the cantilevers was determined using the thermal noise method [29] or the Sader method [30]. Both methods agreed within 10% and values of the spring constants were in the range reported by the manufacturer. Clean glass slides were coated with a layer of PEI in order to adhere the tubes onto the glass surface. During the experiment, individual tubes were compressed and both the force and the deformation of the tube were measured, similar to force–deformation experiments on capsules as described in more detail in Refs. [31,32]. The deformations were limited to deformations in the order of the wall thickness to avoid plasticity and other effects caused by the permeation of solvent through the tube membrane as discussed in Ref. [33].

## 3. Results and discussion

In this paper, a template assisted approach was used to coat readily available glass fibre templates by the Layer-by-Layer technique. The only requirement for the Layer-by-Layer process is a sufficiently high surface charge density of the substrates. For glass fibres to meet this criterion they need only to be cleaned as described in Section 2. After the cleaning

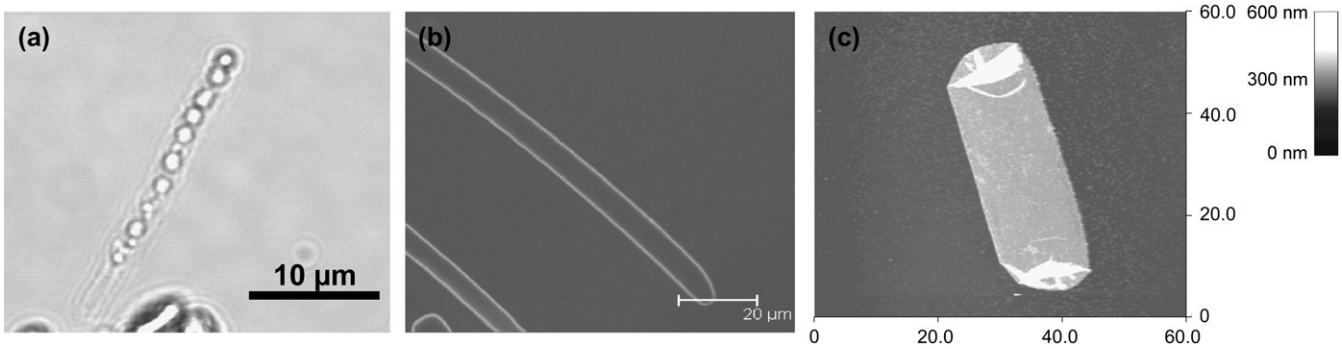


Fig. 1. CLSM image of a $(PDADMAC/PSS)_6$ tube (a) showing a pearling instability after the dissolution of the template and (b) stabilized with an additional layer PAH/PSS, after the dissolution of the template. (c) AFM topography image of a $(PDADMAC/PSS)_6$ tube, as well PAH/PSS stabilized, which is collapsed due to drying.

procedure, six deposition cycles of PDADMAC and PSS were assembled on the template and additionally one layer of PAH/PSS, starting with a PDADMAC layer. Subsequently the fibre substrates were dissolved by exposure to HF solution.

Here, the addition of one PAH layer turned out to be important, because pure PDADMAC/PSS multilayers showed, as displayed in Fig. 1a, a pearling instability upon fibre dissolution. Most likely the instabilities occurred due to the high ionic strength during dissolution, that is known from detailed investigations elsewhere [37] to induce softening of the PDADMAC/PSS multilayers [35]. In contrast, PAH/PSS layers are well known to be stable at high ionic strengths [36], and indeed the instabilities could be suppressed by adding a single layer of PAH. More details on this topic can be found in our recent paper [37]. The obtained hollow fibres were characterized by both Fluorescence Microscopy (after suitable staining as detailed in Section 2) and by Atomic Force Microscopy imaging. The results are compiled in Fig. 1: Confocal Laser Scanning Microscopic images (see Fig. 1b) show that the tubes maintained the diameter and length of the fibres used in the coating process. The wall thickness of the tubes was determined by AFM imaging of the dried tubes (Fig. 1c). Upon drying, the tubes collapsed and the wall thickness was directly measured by step height analysis. Additionally, no height anomalies that would indicate incomplete dissolution of the template fibres were found in our AFM measurements.

The histograms in Fig. 2 compile the data from measurements on a representative number of tubes. If the fibres are broken prior to coating, the length of the tubes was between several tens and a few hundred microns. Here closed hollow tubes were obtained after the Layer-by-Layer assembly, whereas tubes cut after the coating and core dissolution process were open ended (data not shown). The large polydispersity in the tube diameter reflects the polydispersity of the template fibres, and the thickness of the tubes was measured to be slightly larger than the typical range for this material combination [38,39].

One crucial property for the performance of tubes in potential applications is the permeability of the wall material. This property can be probed on an individual tube basis using Confocal Laser Scanning Microscopy: fluorescently labelled probe molecules can be added to the solution and impermeable tubes can be distinguished from permeable ones by the lack of fluorescence in their interior. Fig. 3 shows typical CLSM pictures after addition of fluorescently labelled macromolecules. In the first case, FITC labelled dextran ($M_w = 500\,000$ g/mol), which

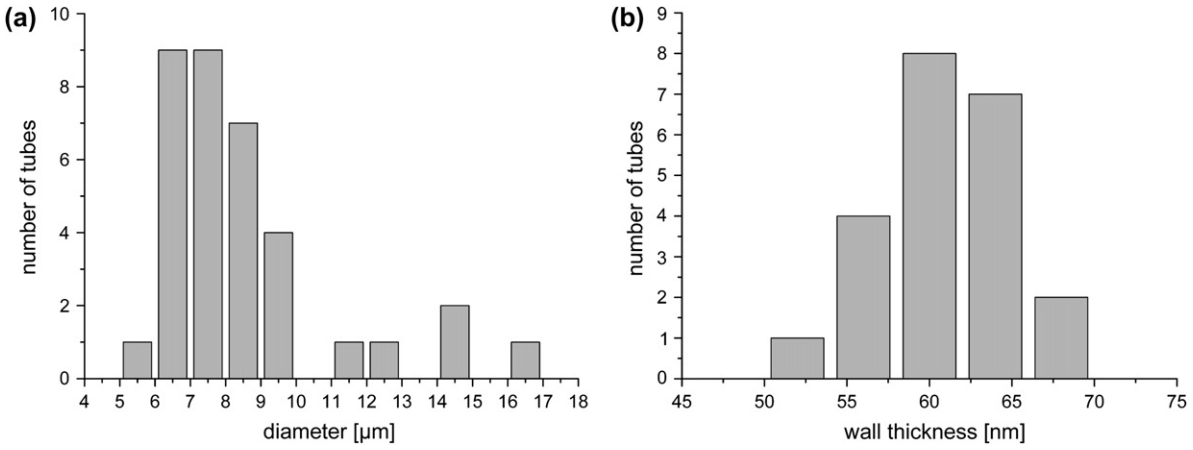


Fig. 2. (a) Histogram of the diameters of the micro-tubes determined with Fluorescence Microscopy and (b) a histogram of their wall thickness as measured with AFM topography imaging.

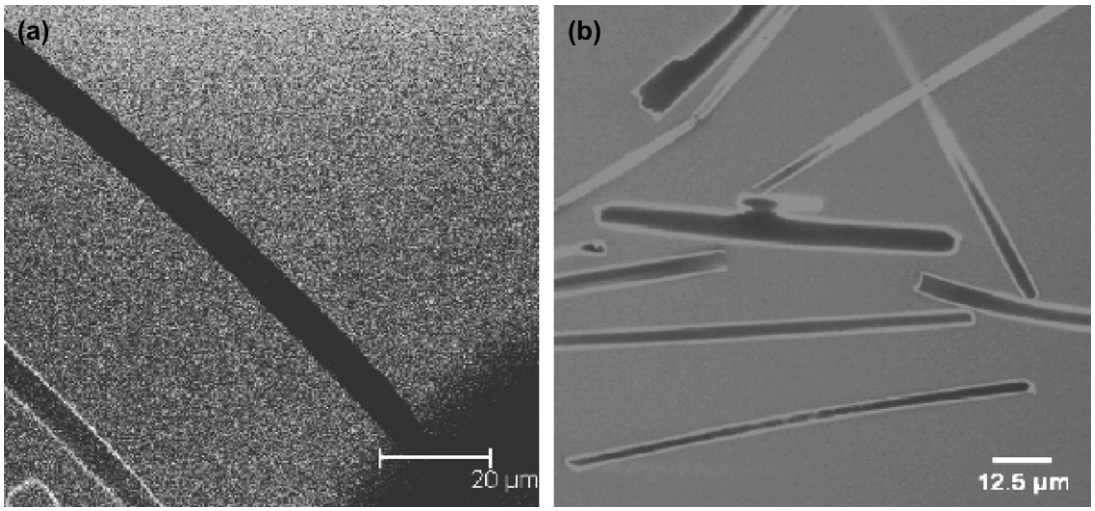


Fig. 3. (a) Defect-free tubes are impermeable for high molecular weight molecules like FITC labelled dextran and (b) they are, as well, impermeable for low molecular weight molecules like Rhodamine, showing an exceptionally defect-free hull. The measurements were performed with CLSM.

is slightly negatively charged due to the fluorescein was added to the sample solution, see Fig. 3a. In the second case, positively charged Rhodamine 6G molecules ($M_w = 479$ g/mol) were added, Fig. 3b. In both examples, the majority (more than 90%) of the tubes showed no fluorescence in their interior. This indicates tube impermeability and an exceptionally defect-free hull. This large amount of defect-free tubes is remarkable and most likely due to the use of glass as the template material. Earlier investigations have shown that the use of polymeric template materials usually results in a much higher risk of defects. The larger molecular weight of the polymeric dissolution products causes osmotic stress on the membrane during dissolution [40,41].

Mechanical properties of the tubes can be determined using AFM Force Spectroscopy. As we have previously demonstrated for hollow polyelectrolyte multilayer capsules, force–deformation properties of such membranes are independent of permeability properties, provided that the deformation remains in the order of the membrane thickness [31]. Mechanical properties of tubes have been previously investigated on microtubules [42] and self-assembled protein nanotubes [25] using similar methods.

All deformation measurements were performed under water and without added salt. As expected, the deformation properties of the tubes were found to be strongly depended on the position along the diameter at which the tube is probed. While in all cases, linear force–deformation behaviour was found for small deformations, the stiffness of the tube varied and increased when the edge of the tube was approached. Close to the edge, instabilities, most likely due to evasion of the tube, were observed (detail information can be found in Ref. [37]). Therefore we probed tubes close to their ‘‘pole region’’. For all measurements, the slope of the force–deformation characteristic was reported, which was called the tubes’ stiffness $c$.

Fig. 4a, a histogram of the measured tubes’ stiffness shows a broad range of stiffness values between a few and almost

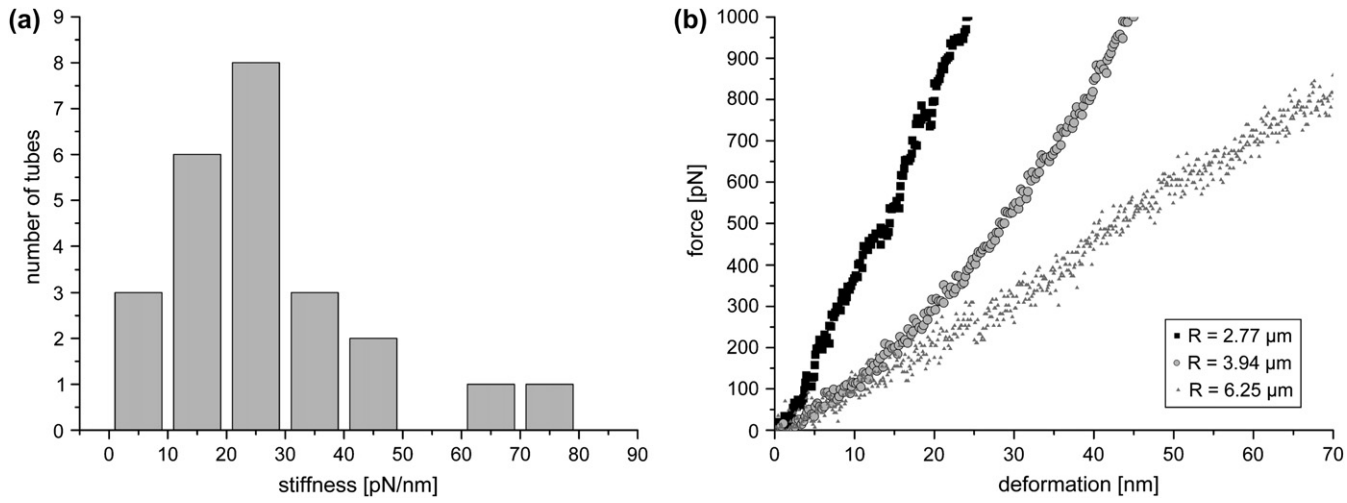


Fig. 4. (a) AFM force spectroscopic measurements were performed in order to obtain a histogram of the stiffness of the tubes. (b) As well, force–deformation curves were taken from tubes with varying diameter (black spots $d = 5.54$ µm, grey spots $d = 7.88$ µm and light grey spots $d = 12.49$ µm).

100 pN/m. Typical force–deformation curves are shown in Fig. 4b. The main control parameter for the tubes' stiffness (and reason for the observed broad range of values) was the radius of the tubes.

The stiffness is found to increase for tubes with smaller radii, which is expected from continuum mechanical considerations as described in Refs. [43,44]. The linear deformation of a curved shell combines an out-of-plane bending and an in-plane compression. Under a point load the cylinder returns to its original shape at a certain distance from the point of force application. For a long, thin-walled cylinder, the softest mode of deformation extends along the axis, for a distance of roughly $R(R/t)^{1/2}$, where $R$ is the tube radius and $t$ is the wall thickness. The deformation perpendicular to the axis extends roughly by $R$. de Pablo et al. [42] found a relation between the deformation, $d$, under the loading force, $F$, and the elastic constant of the wall material, the Young's modulus, $E$:

$$c = \frac{F}{d} \cong 1.18E\frac{t^{5/2}}{R^{3/2}} \quad (1)$$

While the thickness of the tubes, $t$, is assumed to be uniform for the entire sample, the diameter of the tubes scatters due to the polydispersity of the coated fibres. This allows to test the scaling predictions of Eq. (1). Indeed, taking the stiffness values $c$ of the example shown in Fig. 4b, which are 47 pN/nm, 26 pN/nm and 12 pN/nm, one finds that rescaling according to Eq. (2) results in a rescaled stiffness of 0.22 nN($m^{1/2}$), 0.24 nN($m^{1/2}$), and 0.18 nN($m^{1/2}$), respectively.

$$c_{\text{rescaled}} = cR^{3/2} \quad (2)$$

It is worthwhile to mention that the length of the tubes is only important for the deformation properties of the tubes in higher order terms. As long as the length is much larger than the width, the deformation properties like the tubes' stiffness are decoupled from the internal volume of the tube. Thus, tubes of any volume can be easily tailored to give certain deformation properties. This decoupling is not possible for spherical microcapsules where the internal volume is coupled with the deformation properties by the radius of the sphere.

Using Eq. (1), the effective Young's modulus of the wall material, was calculated to be 207 MPa. This result is in-between the values reported in the literature for PAH/PSS (249 MPa) [28] and PDADMAC/PSS (100 MPa) [32]. However, it has to be considered that the calculation is based on a homogenous material, while we have a composite of PAH/PSS and PDADMAC/PSS. This is probably the reason for the slight variances of the rescaled stiffness values above.

## 4. Conclusion

In conclusion, we showed a novel route for the preparation of hollow cylindrical tubes from polyelectrolyte multilayers using the Layer-by-Layer technique on glass fibres and subsequent fibre dissolution. The geometry and wall thickness of the tubes were characterized with Fluorescence Microscopy, Confocal Laser Scanning Microscopy and AFM. The diameter of the tubes reflected the diameter of the glass fibre templates, which was in this case several microns. The wall thickness was in the order of several tens of nanometers and could be easily controlled by changing the number of adsorption cycles during the multilayer assembly. The permeability of the tubes was investigated by Confocal Laser Scanning Microscopy and it was found that the tubes were impermeable to high molecular weight molecules. While this finding is comparable to previous results on microcapsules formed from the same multilayers, a remarkably small fraction of the tubes showed defects. Therefore, this template is particularly well suited for fabrication of tubes with low and controlled permeability because of the low molecular weight of the template's dissolution products. The mechanical properties of the material were determined with AFM Force Spectroscopy of individual tubes. We found that the scaling of the tubes' stiffness with tube radius was described well by continuum mechanical models. These models yield Young's moduli ($E = 207$ MPa) that are compatible with previous measurements. Therefore, these simple models can serve as guidelines for tailoring the tubes' deformation properties, ensuring suitable stability or release by mechanical stimuli.

We believe that these systems can serve as valuable additions to the toolbox of micro- and nano-fluidics. Because they strongly adhere on glass, these tubes can readily be integrated into existing equipment (made from glass). They could act as channels for transport or as mechanical reinforcements. The tubes' well defined permeability properties are beneficial for filtration, sensing and release applications. For the latter field, the independence of deformation properties from encapsulated volume opens new perspectives for tailoring mechanical properties. Identical deformation properties for any encapsulated volume can be achieved by simply selecting a suitable tube length. Previous research has shown that polyelectrolyte multilayers grown on this template material are also stimulus responsive, thus additional applications for these tubes are readily foreseeable.

## Acknowledgements

The authors are grateful to Helmuth Möhwald (MPI, Potsdam-Golm) for valuable discussions and comments, Anne Heilig (MPI, Potsdam-Golm) for AFM imaging, Philippe Carl (Universität Münster) for providing the analysis software PUNIAS and to the Max Planck Society for funding.

## References

[1] Iijima S. Nature 1991;354(6348):56–8.
[2] Ren ZF, Huang ZP, Xu JW, Wang JH, Bush P, Siegal MP, et al. Science 1998;282(5391):1105–7.
[3] Chopra NG, Luyken RJ, Cherrey K, Crespi VH, Cohen ML, Louie SG, et al. Science 1995;269(5226):966–7.
[4] Yager P, Schoen PE. Molecular Crystals and Liquid Crystals 1984; 106(3–4):371–81.
[5] Ghadiri MR, Granja JR, Buehler LK. Nature 1994;369(6478):301–4.
[6] Steinhart M, Wendorff JH, Greiner A, Wehrspohn RB, Nielsch K, Schilling J, et al. Science 2002;296(5575):1997.

[7] Bognitzki M, Hou HQ, Ishaque M, Frese T, Hellwig M, Schwarte C, et al. Advanced Materials 2000;12(9):637–40.
[8] Hou HQ, Jun Z, Reuning A, Schaper A, Wendorff JH, Greiner A. Macromolecules 2002;35(7):2429–31.
[9] Muller K, Quinn JF, Johnston APR, Becker M, Greiner A, Caruso F. Chemistry of Materials 2006;18(9):2397–403.
[10] Decher G, Hong JD. Makromolekulare Chemie-Macromolecular Symposia 1991;46:321–7.
[11] Peyratout CS, Dahne L. Angewandte Chemie International Edition 2004;43(29):3762–83.
[12] Decher G. Polyelectrolyte multilayers, an overview. Wiley-VCH; 2003.
[13] Sukhorukov GB, Fery A, Brumen M, Mohwald H. Physical Chemistry Chemical Physics 2004;6(16):4078–89.
[14] Yang ZH, Yang LL, Bai S, Zhang ZF, Cao WX. Nanotechnology 2006;17(8):1895–900.
[15] Boland ED, Coleman BD, Barnes CP, Simpson DG, Wnek GE, Bowlin GL. Acta Biomaterialia 2005;1(1):115–23.
[16] Qiu XP, Leporatti S, Donath E, Mohwald H. Langmuir 2001;17(17):5375–80.
[17] Dersch R, Greiner A, Steinhart M, Wendorff JH. Chemie in Unserer Zeit 2005;39(1):26–35.
[18] Sanchez-Castillo MA, Couto C, Kim WB, Dumesic JA. Angewandte Chemie International Edition 2004;43(9):1140–2.
[19] Trojanowicz M. TRAC – Trends in Analytical Chemistry 2006;25(5):480–9.
[20] Wang XY, Kim YG, Drew C, Ku BC, Kumar J, Samuelson LA. Nano Letters 2004;4(2):331–4.
[21] Murugan R, Ramakrishna S. Tissue Engineering 2006;12(3):435–47.
[22] Jiang C, Tsukruk VV. Advanced Materials 2006;18(7):829–40.
[23] Huber CA, Huber TE, Sadoqi M, Lubin JA, Manalis S, Prater CB. Science 1994;263(5148):800–2.
[24] Aspnes DE, Heller A, Porter JD. Journal of Applied Physics 1986; 60(9):3028–34.
[25] Graveland-Bikker JF, Schaap IAT, Schmidt CF, de Kruif CG. Nano Letters 2006;6(4):616–21.
[26] Butt HJ. Biophysical Journal 1991;60(6):1438–44.
[27] Ducker WA, Senden TJ, Pashley RM. Nature 1991;353(6341):239–41.
[28] Elsner N, Dubreuil F, Weinkamer R, Wasicek M, Fischer FD, Fery A. Progress in Colloid and Polymer Science 2006;132:117–23.
[29] Hutter JL, Bechhoefer J. Review of Scientific Instruments 1993;64(7):1868–73.
[30] Sader JE. Journal of Applied Physics 1998;84(1):64–76.
[31] Dubreuil F, Elsner N, Fery A. European Physical Journal E 2003;12(2): 215–21.
[32] Mueller R, Kohler K, Weinkamer R, Sukhorukov G, Fery A. Macromolecules 2005;38(23):9766–71.
[33] Fery A, Dubreuil F, Mohwald H. New Journal of Physics 2004;6:18–31.
[35] Jaber JA, Schlenoff JB. Journal of the American Chemical Society 2006;128(9):2940–7.
[36] Heuvingh J, Zappa M, Fery A. Langmuir 2005;21(7):3165.
[37] Mueller R, Daehne L, Fery A. Journal of Physical Chemistry B, accepted for special issue on Polyelectrolytes.
[38] Caruso F, Niikura K, Furlong DN, Okahata Y. Langmuir 1997;13(13): 3422–6.
[39] Dubas ST, Schlenoff JB. Macromolecules 1999;32(24):8153–60.
[40] Moya S, Dahne L, Voigt A, Leporatti S, Donath E, Mohwald H. Colloids and Surfaces A – Physicochemical and Engineering Aspects 2001;183:27–40.
[41] Dai ZF, Dahne L, Donath E, Mohwald H. Langmuir 2002;18(12):4553–5.
[42] de Pablo PJ, Schaap IAT, MacKintosh FC, Schmidt CF. Physical Review Letters 2003;91(9). 0941011-0091014.
[43] Landau LD. Theory in elasticity. Butterworth-Heinemann; 1986.
[44] Niordson FI. Shell theory. Amsterdam: North-Holland; 1985.